Nucleation Stages Onset and Intra-granular Ferrite Morphologies in Titanium Free Micro-Alloyed Steel

Abdulnaser Hamza Fadel
Al Zawia University, Faculty of Natural Resources

Email: Naser.fadel2369@gmail.com
Al Zawia, Libya

Nenad Radović
University of Belgrade, Faculty of Technology and Metallurgy, Department of Metallurgical Engineering
Karnegijeva 4, 11120 Belgrade, Serbia

Abstract —**The aim of this work is focused on nucleation stages with emphasis on the development of intra-granular ferrite morphologies during isothermal austenite transformation in titanium free micro-alloyed steel. Isothermal treatment was carried out in the temperature range 350 to 600^{o}C. These treatments were interrupted at different times between 2 and 1800 s in order to analyze the evolution of the microstructure. Metallographic evaluation was done by using optical and scanning electron microscopy (SEM) enabled determination of the nucleation onset at all treatments and subsequent on the development of intra-granular ferrite of isothermally treated Ti free micro-alloyed steel. The results show that at high temperatures (≥ 500 ° C) polygonal intra-granularly nucleated ferrite idiomorphs, combined with grain boundary ferrite and pearlite were produced and followed by an incomplete transformation phenomenon, At intermediate temperatures (450 and 500 ° C) an interlocked acicular ferrite (AF) microstructure is produced, and at low temperatures (400 and 350 ° C) the sheave of parallel acicular ferrite plates, similar to bainitic sheaves but intra-granularly nucleated were observed. In addition to sheaf type acicular ferrite, the grain boundary nucleated bainitic sheaves are observed.**

Index Terms: **Micro-alloyed steel, Grain Boundary Ferrite, Bainitic Sheaves, Acicular ferrite, Widmanstatten ferrite, Polygonal ferrite, pearlite.**

I. INTRODUCTION

Ferrite formation during austenite decomposition can result in obtaining two different morphologies: (i) diffusion controlled (allotriomorphic and idiomorphic) or (ii) displacive (Widmanstätten and Intragranular plates) [1-5]. Allotriomorphic ferrite nucleates at the prior austenite grain boundaries and tends to grow along the austenite boundaries at a rate faster than in the perpendicular direction to the boundary plane.. By contrast idiomorphic ferrite nucleates at the inclusions/particles the inclusions/particles inside the austenite grains and can be identified in the microstructure by its equiaxed polygonal morphology. Therefore, the balance between the number of intra-granular nucleation sites and the number of sites at the austenite grain boundaries is a very important factor in the competitive process of allotriomorphic-idiomorphic ferrite formation. The prior austenite grain size exerts an important influence on the decomposition of austenite [5, 6]. An increase in austenite grain size leads to a reduction in the number of nucleation sites at the austenite grain boundaries indirectly favoring the intra-granular nucleation of ferrite, i.e. the formation of idiomorphic ferrite, rather than allotriomorphic ferrite. In order to obtain bainite, the austenite grain size has to be small so that nucleation from grain boundaries dominates and subsequent growth then swamps the interior of the austenite grains. By contrast acicular ferrite is nucleated intra-granularly on inclusions within large austenite grains and then radiates in many different directions. The presence of a uniform layer of allotriomorphic ferrite along the austenite grain boundaries induces the transformation of austenite in acicular ferrite instead of bainite [1, 3-6]. The acicular ferrite is in fact intra-granularly nucleate bainite [4-6]. It is a much more disorganized microstructure with a larger ability to deflect cracks. Acicular ferrite is therefore widely recognized to be a desirable microstructure due to good mechanical properties [5]. Data related to nucleation phase of isothermal decomposition seems to be lacking; most of the published results deal with later steps (10s or longer), i.e. when the nucleation is well prolonged. Therefore, the aim of the present study is to clarify experimentally the nucleation stages onset at higher, intermediate and lower isothermal temperature treatment. Moreover the influence of isothermal transformation temperature and time on the nucleation of intra-granular ferrite and indirectly, on the development of the intra-granular acicular ferrite in titanium free micro-alloyed forging steel has been investigated.

Received 2 March 2017; revised 26 March 2017; accepted 19 April 2017.

Available online 20 April 2017.

II. EXPERIMENTAL

The steel used for this investigation was made by full-scale casting and fabricated into 19mm diameter bar by full-scale forging and hot-rolling. Representative hot-rolled steel bars were homogenized at 1250^{o} C for 4 hours, in the presence of argon as protective atmosphere, to minimize any effect of chemical segregation. After annealing, the samples were water quenched, and then the specimens with 12mm length were cut from 19 diameter bars and austenitized at 1100 ^{o} C for 10 min in an argon atmosphere. After austenitization, specimens were isothermally transformed at different temperatures ranging from 350^{o} C to 600^{o} C at different times between 2 and 1200 s. Finally, specimens were water quenched to room temperature. The samples were cut, mechanically ground and then polished to 1µm diamond finish paste using standardized metallographic techniques and subsequently etched in 2 % nital for their observation by optical and scanning electron microscopy (SEM). The samples were used to reveal grain boundaries by thermal etching based on the combination of heat treatment and thermal etching (TE) method [26, 27]. The prior austenite grain size generated by austenitizing at 1100 ^{o} C for 10 min was determined using a linear intercept technique and found to be 67 ±3µm. The chemical compositions by (wt%) of tested steel are given in Table 1.

Table 1: Chemical Composition of the Experimental Steel

C	Si	Mn	P	S	Cr
0.256	0.416	1.451	0.0113	0.0112	0.201
Cu	Al	Mo	Ti	V	N
0.183	0.038	0.023	0.002	0.099	0.0235

III. RESULTS AND DISCUSSION

Dissolution Temperature

The equilibrium temperatures for complete dissolution of VN in present steel was calculated according to the equation given in Ref. [28], and it was estimated to be 1100^{o} C.

Prior Austenite Grain Size (PAGS)

The experimental results of the PAGS for this steel by austenitizing at 1100 ^{o} C for 10 min is 67 ±3µm, and is expected to enhance intra-granular AF formation rather than bainite by increasing the ratio between intra-granular and grain boundary sites [29, 30].

Nucleation Onset Time

The experimentally determined nucleation onset time is presented in table 2. The Grain Boundary Ferrite (GBF) the first phase to nucleate over the entire temperature range tested, is shown in Figures 2(a-e) and is represented by a two types of transformation, describing the effect of temperature on nature of transformation.

Table2. The experimentally phases observed and determined nucleation onset time of steel investigated.

Temperature by ^{o} C	Phases observed				R_f
	GBF	IGF	BS	P	
350	7	Nil	10	Nil	600
400	2	Nil	20	Nil	600
450	2	Nil	Nil	Nil	1200
500	3	10	Nil	80	> 1200
550	5	20	Nil	45	> 1200
600	7	30	Nil	30	> 1200

R_f is transformation finish time by second

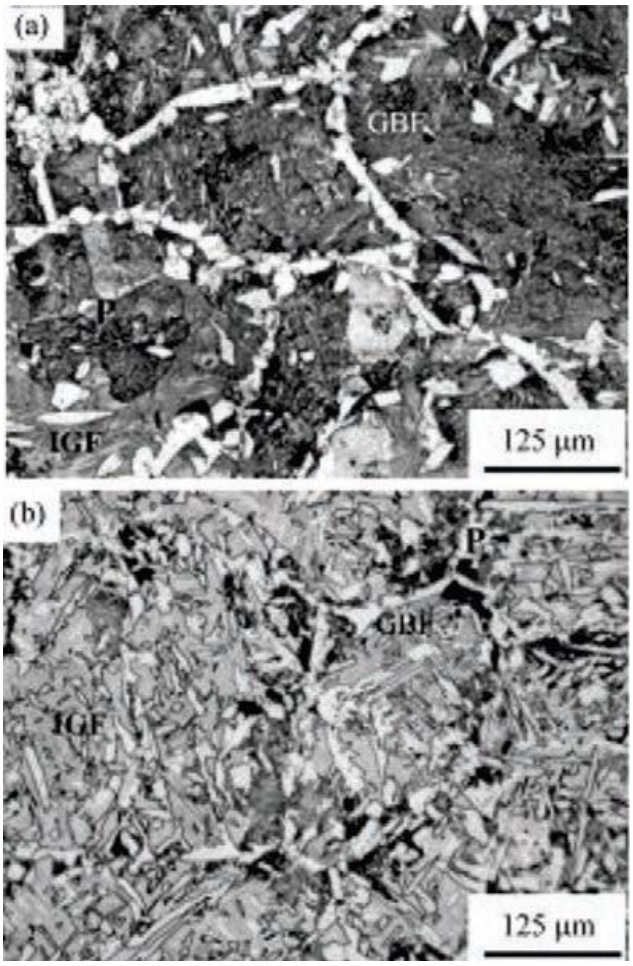

Fig. 1. (a, b) .Optical Micrographs Showing Microstructures and Population Density Obtained after 120s of is Othermal Treatment at High Temperature (a) 600 ^{o} C, (b) 550 ^{o} C

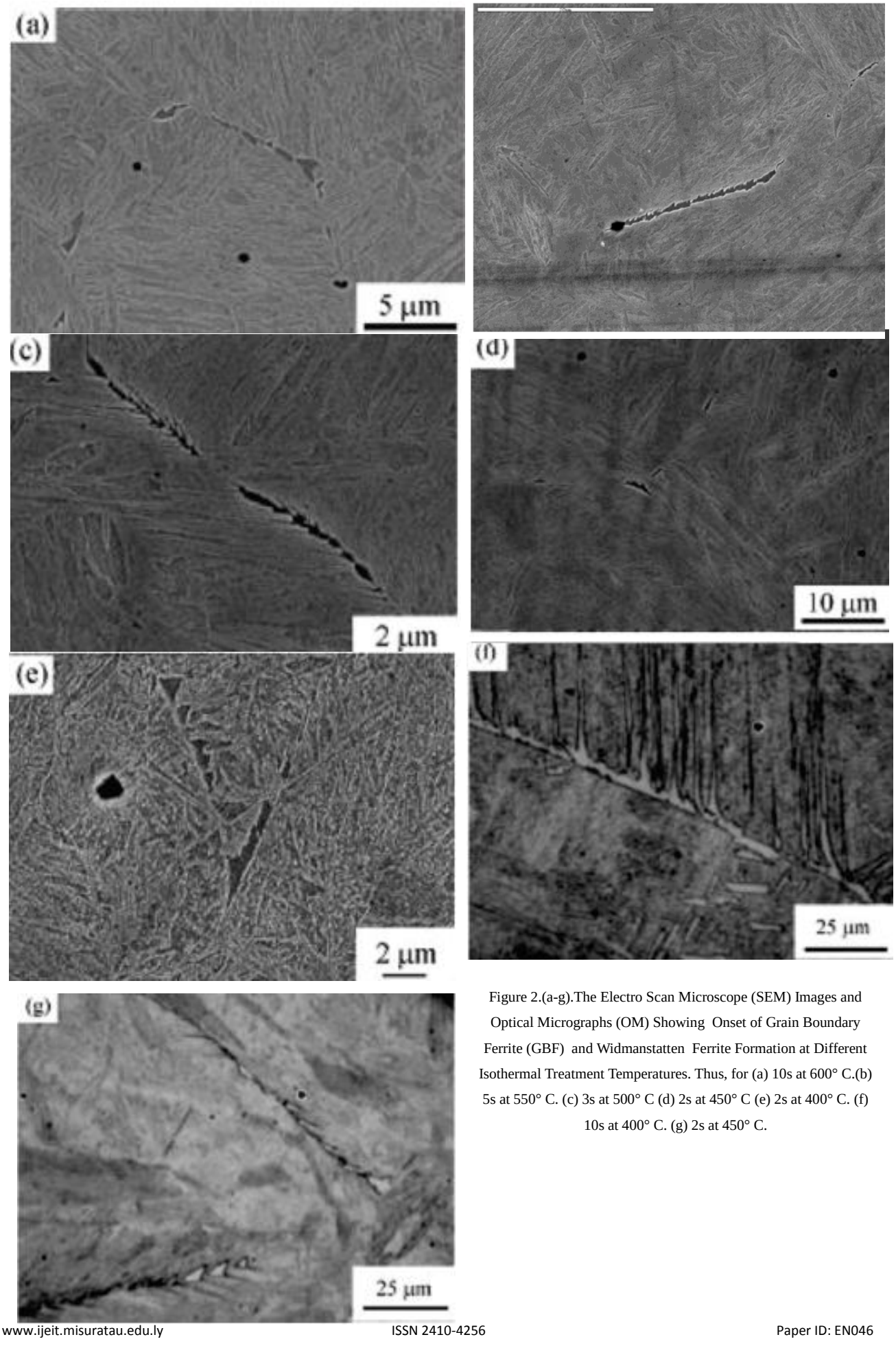

Figure 2.(a-g).The Electro Scan Microscope (SEM) Images and Optical Micrographs (OM) Showing Onset of Grain Boundary Ferrite (GBF) and Widmanstatten Ferrite Formation at Different Isothermal Treatment Temperatures. Thus, for (a) 10s at 600° C.(b) 5s at 550° C. (c) 3s at 500° C (d) 2s at 450° C (e) 2s at 400° C. (f) 10s at 400° C. (g) 2s at 450° C.

Diffusional Transformations

Figures 2(a-e) is represented by electro scan microscope (SEM) images and optical micrographs (OM) describing the effects of diffusional and displacive transformations. Within the lower temperature a clear indication of Widmanstatten nucleation is observed Figure 2(f,g). At a later stage the different intra-granular ferrite (IGF) morphologies are initiated, what is represented again by (IGF) nucleation onset time in table 2. In the (IGF) region, three different morphologies have been observed depending upon the isothermal treatment temperature.

Firstly, at upper or high temperatures ($\geq 550^{o}$ C) intra-granularly nucleated ferrite combined with grain boundary ferrite (GBF) and pearlite (P) are produced, as shown in figure 1(a,b). The intra-granular ferrite is characterized by polygonal idiomorphic (IGF) ferrite. The idiomorphic ferrite nucleates intra-granularly at the inclusions distributed inside the austenite grains, and the volume fraction of idiomorphic ferrite is related to the volume fraction of inclusions in steel [31]. The transformation after 1200s of isothermal treatment at 550 and 600 ^{o} C reveals that a fraction of austenite remains untransformed, Fig. 3(a,b). This phenomenon has been described by Bhadeshia [16, 32-34] and is known as incomplete reaction phenomenon. At 600 ^{o} C, there was thicker grain boundary ferrite than at 550 ^{o} C, but in respect to the population density of ferrite plates inside the prior austenite grains it is lower as can be seen in Fig.1 (a,b). This seems to indicate that at 600 ^{o} C, the carbon rejected from the ferrite plates diffuses rapidly leading to super saturation in austenite. The carbon enrichement of the remaining austenite together with relatively small driving force for transformation at 600 ^{o} C is enough to inhibit the formation of new ferrite plates [32].

Acicular Ferrite Transformation

The second type of intragranular ferrite morphologies occur at intermediate temperature (450 and 500 ^{o} C). An interlocked acicular ferrite (AF) microstructure is produced as can be seen in Fig.4 (d). At the initial stages, the nucleation of the primary ferrite plates takes place intra-granularly at second phase particles (nonmetallic inclusions) present in the austenite, as can be seen in figure 4 (a,b), which is in good agreement with [14, 16, 17, 24, 31, 32]. The micrograph present in Figure 4(c) and an energy dispersive X-ray (EDX) spectrum analysis illustrate a typical active inclusion, with the corresponding chemical analysis at different points of the

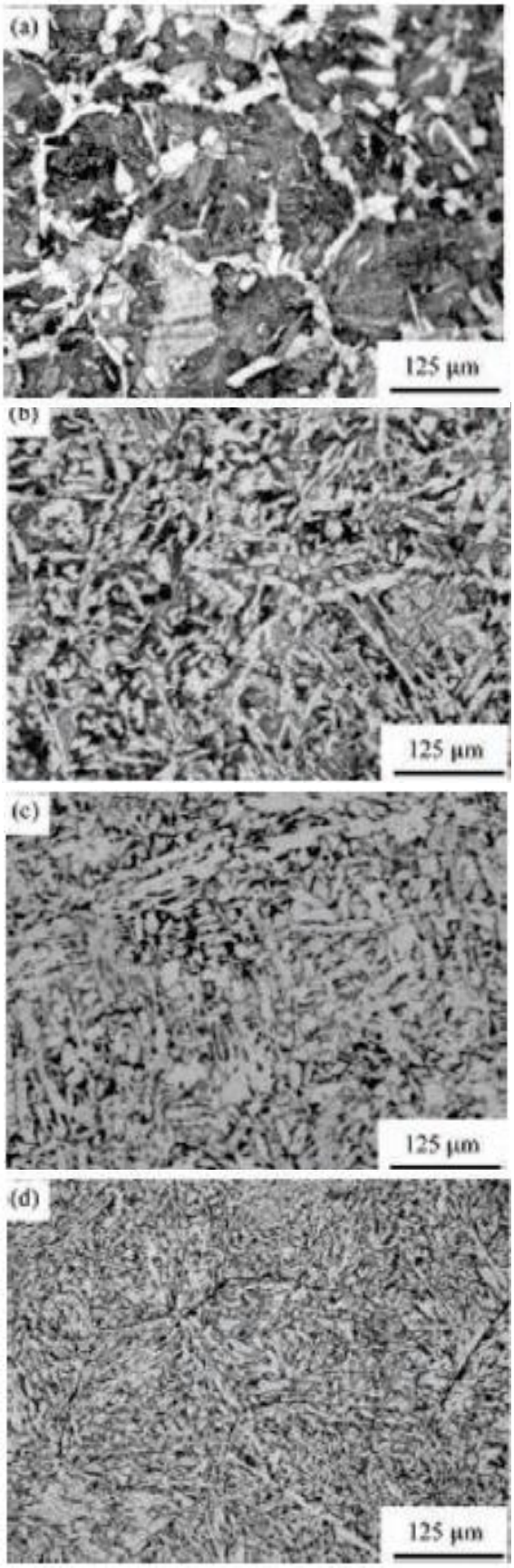

Figure3.(a-d).Optical micrographs showing the microstructures after 1200s of isothermal transformation temperatures .Thus, for (a) 600 ^{o} C (b) 550 ^{o} C (c) 500 ^{o} C (d) 450 ^{o} C

.

particle, it is identified as Ca treated manganese sulfidesinclusion core covered or at least partially covered with VN or V(C, N) complex precipitate. This is in good agreement with results reported by Ochi et al and Ishikawa et al. [34, 35]. The manganese sulfides have been reported previously to be active on nucleating acicular ferrite [8, 10, 23, 24, 31, 34, 36]. Moreover the inclusion size and shape is modified by Ca treatment (Morphology altered by Ca addition - in order to control and modify the shape of MnS inclusions, i.e. to get spherical shape and very low deformability). The majority of MnS inclusions in the Ca-treated steels were globular (Ca, Mn)S particles. MnS particles represented the largest contribution (60-70%) to the overall inclusion volume fraction [37]. However the nucleation of AF plates is not restricted to inclusions, new ferrite plates can grow from pre-existing ones, as can be observed in Figure 5 (b), which supports the view, that nucleation occurs sympathetically. In Figure 5(b), the sympathetic nucleation of secondary acicular ferrite plates has been observed to occur at the austenite/primary acicular ferrite interface and continue to grow within the austenite matrix until impingement occurs with other plates. An example of impingement processes is illustrated in the SEM micrographs as clearly shown in Figure 5(c). The result of multiple sympathetic nucleation is an interlocking ferrite network, and after sufficient time, it results into a complex interlocking ferrite microstructure, characteristic of acicular ferrite, such as that shown in Fig. 4(d). The resulting microstructure with fully acicular ferrite structure in medium carbon micro-alloyed steel, with the exception of a few small bainitic zones is in good agreement with published data [8]. However the present results clearly show no carbides were observed to form within the ferrite plates at intermediate time and temperature (450-500 ^{o} C) as can be seen in Fig. 4(c). This is good a greement with published data [16, 23, 32]. The incubation time is the shortest time at which it was possible to find grain boundary ferrite, and it is found to be approximately at 400 - 450°C (Table and figure 2). The maximum acicular ferrite content in the present steel is found for treatment carried out at 450°C. This treatment is characterised by the fully acicular ferrite formation. On the other hand, it is possible to find, in certain localized places, bainite formed at the grain boundaries, as shown in Figure 5(d). At 450-500 ^{o} C, the majority of plates are free of precipitates due to the carbon diffusion is high, favouring the decarburisation of the majority of ferrite plates, as can be seen in Fig. 4(c).

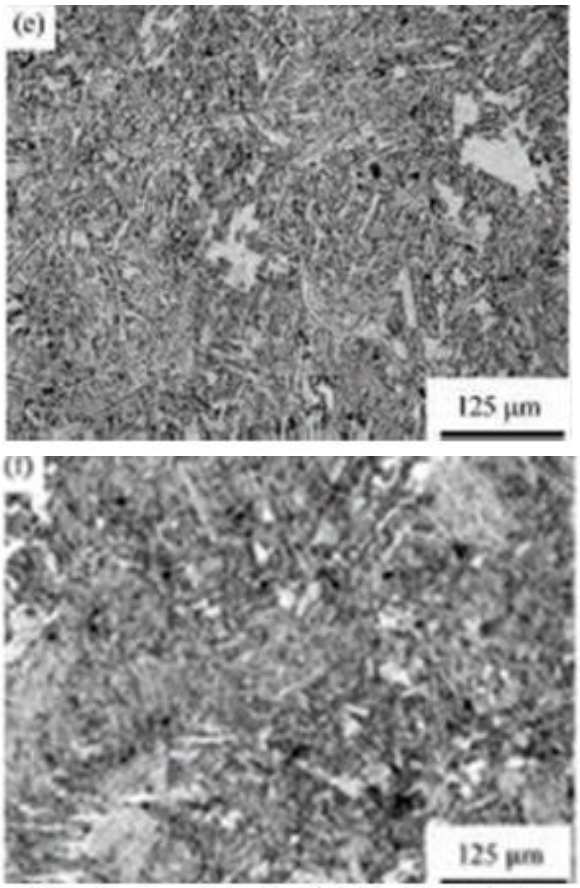

Fig.3. Continue. For (e) 400 ° C and (f) 350° C.

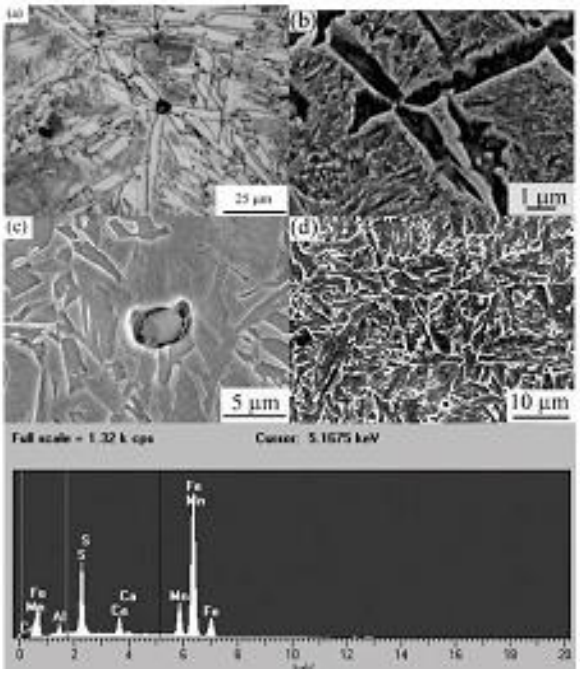

Figure 4. (a,b) Optical micrographs and SEM image showing onset of acicular ferrite on inclusion after (a) 30s at 500°C. (b) 20s at 450 ^{o} C. (c) SEM image and EDX spectrum showing the type of inclusion exist. 5(d) SEM image showing the acicular ferrite microstructure after 1200s at 450 ^{o} C.

Pearlitic Transformation

The onset of pearlite at different a treatment temperature ($\geq$ 500 ^{o}C) is illustrated in Figure 6 (a-d) and it is found to be equal 30, 45 and 80 second (table 2).

Bainitic and Martensitic Transformation

The bainitic transformation start temperature (BS) in the present study was calculated by use of different empirical formulas [16, 38-41] and it is found to be equal 530 ± 10 ^{o}C. However the martensite– start (MS) temperature is experimentally determined. The results show that it occures close to 330 ^{o}C. This result is in good agreement with martensite – start (MS) temperature calculated by different empirical equations [41-45].

Displacive Transformations

The third type of intra-granular ferrite morphology exists at low temperatures (350, 400^{o} C). Two different morphologies are present at the beginning of the transformation, Bainite sheaves BS as can seen in figure 7(a) and interlocked AF as can seen in Figure 7(b).The origin of Bainitic sheaves are exclusively the grain boundaries. The nucleation of Bainitic Sheaves is indicated in table 2. by BS symbol. When the isothermal treatment times is increased a new intra-granular morphology known as the sheaf type acicular ferrite (STAF) [23] is observed as can be seen in Figure 7(c). There is tendency to form sheaves composed of parallel plates but the nucleation does not take place at the grain boundaries. The transition between an interlocked morphology and sheaf type morphology was estimated to occur at 450/400 ^{o}C. This morphological transition can be related to the transition from upper to lower acicular ferrite and to differences in the carbon concentration profiles in the parent austenite in the front of the interface of the primary acicular plates depending on the treatment temperature. As it is suggested [22,23], at initial stages for the transformation at 400°C, the carbon concentration in austenite close to the tips of primary plates is lower than at the faces (side direction). Therefore, instead of growth in side direction, nucleation on the tips of present sheaf is favored, due to carbon enrichment on side direction. Overall, in final microstructure sheaf type AF dominates on the expense of interlocked type [22,23]. Whereas at 450 ^{o}C the stronger diffusion of carbon from the austenite/ferrite interfaces makes possible the plate nucleation on faces i.e the carbon is able to diffuse away from the austenite / ferrite interfaces in shorter times than at 400 ^{o}C. This is expected to allow the nucleation of new ferrite variants on the primary plate faces in agreement

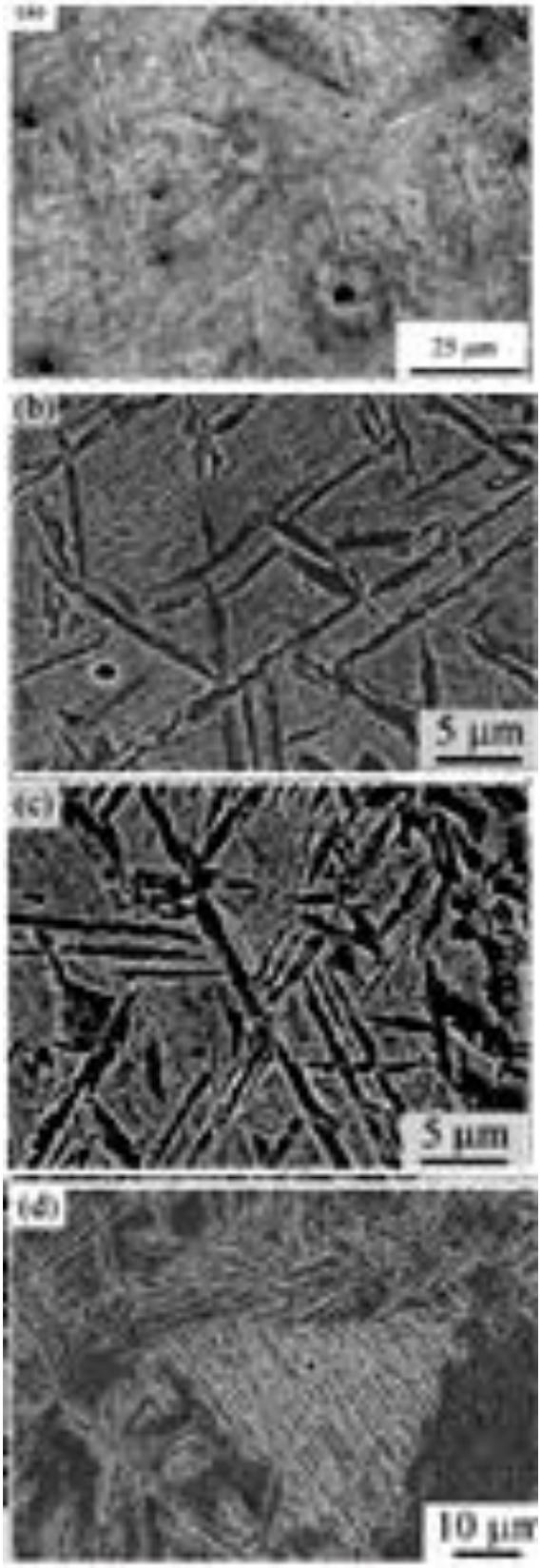

Figure. 5 (a) OM image after 10s at 450 ^{o}C; (b, c) SEM image after 20s at 450 ^{o}C (d) SEM image showing an isolated bainite area formed in the steel sample treated for 30s at 450 ^{o}C.

with interlocked plate microstructure obtained at 450 ^{o}C , as seen in Figures 5(b), 4(d) and 3(d).

Final Microstructures

Microstructures in Figures 3(a-f) are obtained after 1200s of isothermal treatments at 350, 400, 450, 500, 550 and 600 ^{o}C. They refer to the competition of transformation (R_f finish line in table 2.). At temperature ≥ 550 ^{o}C, the austenite has been transformed into a mixture of allotriomorphic and idiomorphic ferrite and pearlite. However, some of the austenite remains stable, and only after the final water quenching it transforms to martensite as shown in Figure 1 (a,b). At 500 ^{o} C, some small colonies of pearlite have been formed between the acicular ferrite plates as shown in Figure 8(a,b). As the transformation temperature is reduced to 450 ^{o} C, the refinement of the ferrite plate is achieved (a great number of adjacent ferrite plates present) as shown in Figure 3 (d).and 4(d). In this case, the austenite has transformed to acicular ferrite, giving rise to the characteristic interlocked microstructure as seen in Fig. 4(d).As temperature is decreased to 400 and 350 ^{o}C, mainly two morphologies are observed BS and sheaf type acicular ferrite, as demonstrated in Fig. 7(c).

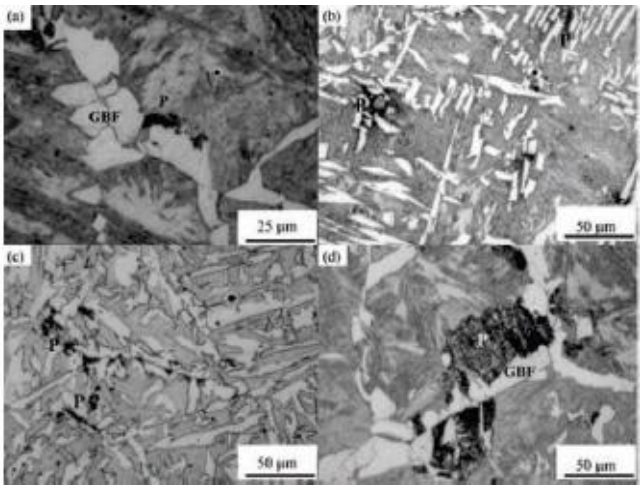

Figure 6. (a-c) Optical micrographs showing the pearlite onset at (≥ 500 ^{o}C). (a) 30s at 600 °C. (b) 45s at 550 °C. (c) 80s at 500 °C (d) Optical micrograph showing intragranulary nucleated ferrite combined with grain boundary ferrite (GBF) and pearlite (P) at 600 ^{o}C for 60s as isothermal time.

IV. CONCLUSIOS

Isothermal decomposition of medium carbon vanadium micro-alloyed austenite was evaluated by optical and SEM metallography. Four constituents are found to be relevant to this of transformation.

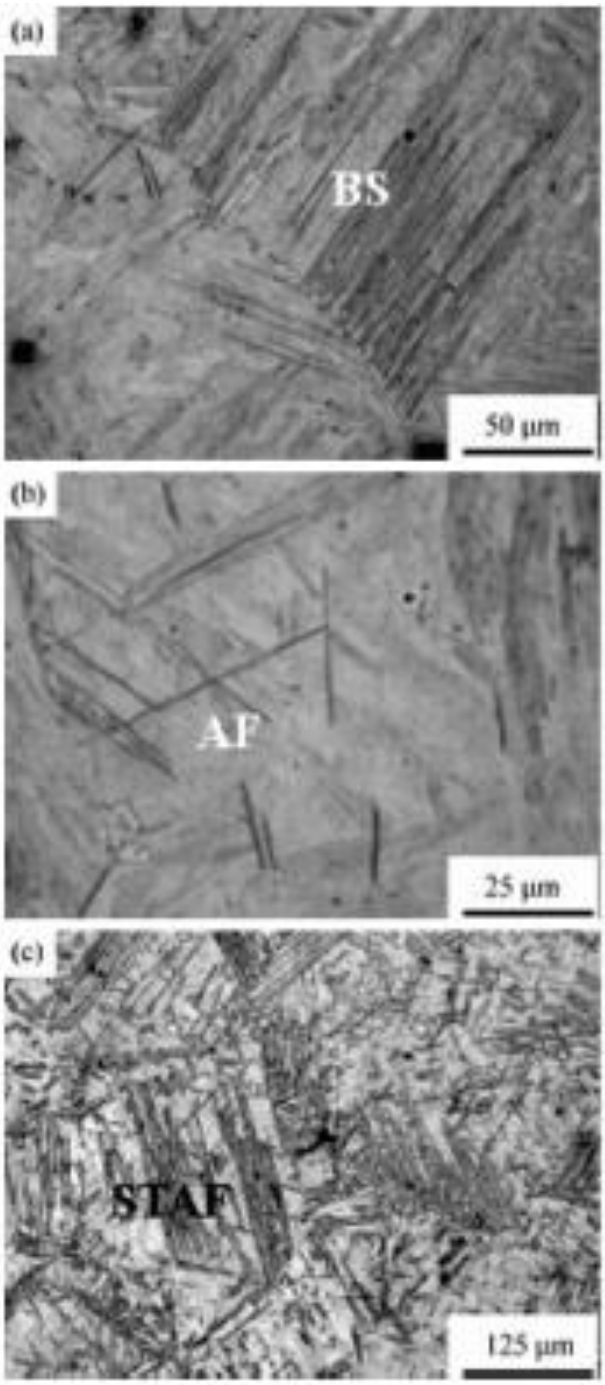

Fig.ure 7 (a ,b) OM showing BS and AF onset after 10s of isothermal treatment at 350 °C respectively and 7 (c) OM showing BS and STAF formation after 20s of treatment at 350°C.

(1) Grain boundary ferrite is the first phase to be generated at all temepratures. In the lower temperature range the widmanstetten ferrite is formed, while on higher temperatures grain boundary allotriomorphs are produced. This difference is attributed to displacive

nature of transformation at lower and. diffusional transformation at higher temperatures.

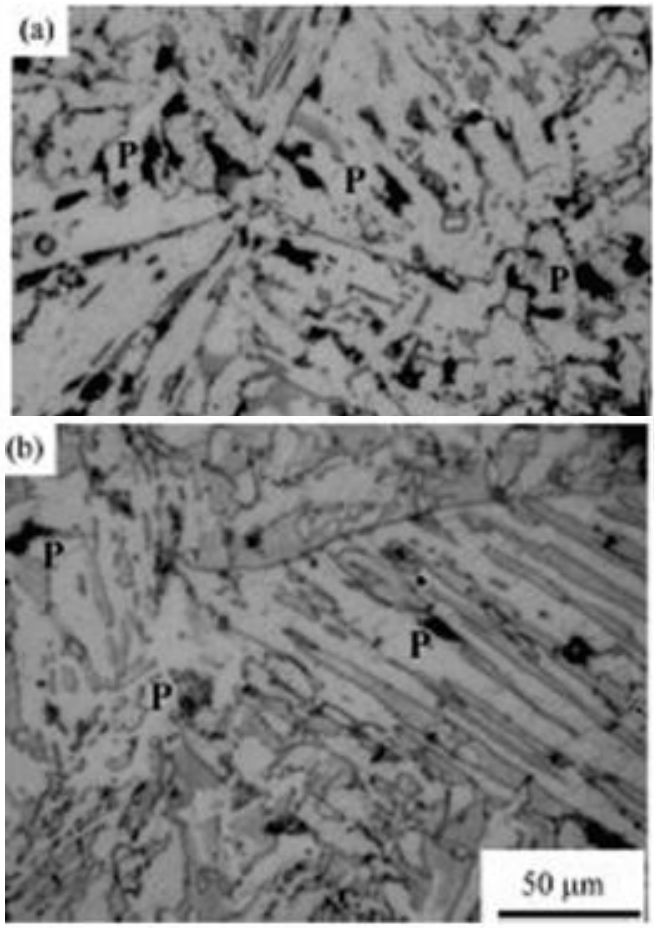

Figure. 8 (a, b) Optical micrographs showing some small Colonies of pearlite formed between the acicular ferrite plates at 500°C after. (a) 600s.and (b) 240s of isothermal treatment .

(2) Second constituent is related to nucleation of intra-granular ferrite (IGF). In the lower temperature range (350–400 ^{o} C) acicular ferrite plates are grouped in sheaves; at intermediate temperatures (450–500 ^{o} C), a more interlocked microstructure of acicular ferrite was clearly obsorved, while microstructure generated at high temperatures (550–600 ^{o} C) is characterized by polygonal idiomorphic ferrite.

(3) Third constituent is related to onset of pearlite. It occurs at temperatures 500 ^{o} C, followed by an incomplete reaction phenomenon.

(4) The transition between an acicular ferrite sheaf morphology and interlocked microstructure is observed to take place at 400/450 ^{o} C. However the bainitic sheaves are frequently observed when the isothermal transformation time is increased at 400 ^{o} C, and temperature diminishes to 350 ^{o} C .

(5) Finish of transformation was clearly observed at temperatures below 500 ^{o} C. However at 550 and 600 ^{o} C, incomplete reaction phenomenon occurs. This behaviour is attributed to carbon enrichment in austenite and decrease of driving force for austenite decomposition.

REFERENCES

[1] G. Krauss, S.K. Banerji (Eds.), Fundamentals of Microalloying Forging Steels, The Metallurgical Society TMS,Warrendale, PA, USA,1987, p. 55.
[2] P.E. Reynolds, Heat Treat. Met. 3 (1990) 69 -72.
[3] M.A. Linaza, J.L. Romero, J.M. Rodrıguez-Ibabe, J.J. Urcola: Scripta Met. Mater. 29 (9) (1993) 1217–1222.
[4] I. Madariaga, I. Gutierrez, Materials Science Forum., 284-286 (1998) 419-426.
[5] M.A. Linaza, J.L. Romero, J.M. Rodrıguez-Ibabe, J.J. Urcola, Scripta Met. Mater., 32 (3) (1995) 395–400.
[6] A. Echeverria, J.M. Rodrıguez-Ibabe, Scripta Mater., 41 (2) (1999) 131–136.
[7] M.J. Balart, C.L. Davis, M. Strangwood, Mater. Sci. Eng., A284(2000) 1–13.
[8] I. Madariaga, J. L. Romero, and I. Gutierrez: Met. And Mat. Tran ., 29 A (1998) 1003-1015.
[9] Garcia de Andres, C., Capdevila, C., Caballero, F.G., & D San Martin. J.of Mat. Sci., 36 (2001) 565-571.
[10] I. Madariaga and I. Gutierrez: Acta mater., 47 (3) (1999) 951-960.
[11] I. Madariaga and I. Gutierrez : Scripta mater., 37 (8) (1997) 1185-1192.
[12] M. Dıaz-Fuentes, I. Madariaga, J.M. Rodrıguez-Ibabe, and I. Gutierrez: J.Construct, Steel Res., 46 (1-3) (1998) 413-14.
[13] D. Glisic, N. Radovic, A. Koprivica, A. Fadel and D.Drobnjak: ISIJ Int., 50 (4) (2010) 601–606
[14] S.S. Babu and H.K. D. H. Bhadeshia: Mat. Trans., JIM 32 (8) (1991) 679-688.
[15] M.J. Perricone: Bainitic Structures, Metallography and Microstructures, Metals Park, OH, ASM International, USA 2004, p.179.
[16] H.K.D.H.Bahdeshia: Bainite in Steels, The Institute of Materials, London, 2001, p.237.
[17] A. Khodobandeh, M. Jahazi, S. Yue and P. Bocher: ISIJ Int., 45 (2) (2005) 272-280.
[18] C. Capdevila, J. P. Ferrer, C. Garcia-Mateo, F. G. Caballero, V. Lopez and C. G. DeAndres: ISIJ Int., 46 (7) (2006) 1093-1100.
[19] C. Garcia-Mateo, C. Capdevila, F. G. Caballero, C. G. DeAndres: ISIJ Int., 48 (9) (2008)1270-1275.
[20] G. I. Rees and H.K. D. H. Bhadeshia: Mat. Sci. and Tech.,10 (1994) 353.
[21] S.S. Babu and H.K.D.H. Bhadeshia: Mat. Sci. and Tech., 6 (1990) 1005-1020.
[22] I. Madariaga, I . Gutierrez, C. G. Deandres and C. Capdevila: Scripta Mater., 41 (1999) 229.
[23] I. Madariaga, I. Gutierrez, H.K.D.H. Bhadeshia: Metall. Trans., A 32A (9) (2001) 2187-2197.
[24] T. Furuhara, T. Shinyoshi, G. Miyamoto, J. Yamaguchl, N. Sugita, N. Kimura, N. Takemura and T. Maki: ISIJ Int., 43 (12) (2003) 2028-2037.
[25] C. G. De Andres, C. Capdevila, D. San Martin and F. G. Caballero : J. of Mat. Sci., 20 (2001) 1135 –1137.
[26] C. Garcia de Andres, F.G. Caballero, C. Capdevila, D. San Martin : Mater. Charact., 49 (2003) 121-127.
[27] C. Garcia de Andres, M.J. Bartolome, C. Capdevila, D. San Martin, F.G. Caballero and V. Lopez: Mater Charact., 46 (2001) 389-398. [28] H. Adrian: Proc. of Int. Conf. Microalloying '95, ISS, Warrendale,PA, USA,1995, p. 285.
[29] C. Capdevila, F. G. Caballero. C. Gracia-Mateo and C. Garcia de Andres: Mater. Trans., 45 (2004), 2678.
[30] C. Capdevila, F. G. Caballero, and C. Garcia de Andres: Mater. Sci. Technol., 19 (2003) 195-201.
[31] C. Capdevila, F.G. Caballero, and C. Garcia de Andres: Met. and Mat. Trans.A., 32A (2001) 1591-1597.
[32] M. Dıaz-Fuentes, I. Gutiérrez: Mat. Sci and Eng., A363 (2003) 316-324.

[33] H. K. D. H. Bhadeshia and D.V.Edmonds: Metall. Trans., A10 (1979) 895-907.
[34] T. Ochi, T. Takahashi and H. Takada: Mechanical Working and Steel Processing Conf. Proe. , ISS-AIME, Warrendale, PA,USA, 1988, p. 65-72.
[35] F. Ishikawa, T. Takahashi, T. Ochi: Metall. Mater. Trans., 25A (5) (1994) 929-936..
[36] S. Zajac: Mat. Sci. Forum., 500-501(2005) 75-86.
[37] M.J. Balart, C.L. Davis, M. Strangwood: Mat. Sci. And Eng., A328 (2002) 48-57.
[38] Z. Zhao, et al: Journal of Materials Science., 36 (2001) 5045-5056.
[39] H.K.D.H. Bhadeshia and R.W.K.Honeycombe: Steels Microstructure and Properties, Elsevier Ltd, London 2006, p.147.
[40] Y. K. Lee: J. of Mat. Sci. Letters., 21(2002) 1253 1255.
[41] Antonio Augusto Gorni: Steel Forming and Heat Treating Handbook, São Vicente, Brazil 2011, p.24.
[42] J. Wang, P. van der Wolk and S. van der Zwaag: Mater. Trans., JIM, 41(7) (2000) 761-768.
[43] B. Mintz, The influence of aluminium on the strength and impact properties of steel, Int. Con. on TRIP-aided H. S. Ferrous Alloys, Ghent, Belgium, 2002, p. 379- 382
[44] S. Chupatanakul, P. Nash, and D. Chen: Met. And Mat. Int.,12 (2006) 453-458.
[45] M. Arjomandi, H. Khorsand, S. H. Sadati and H. Addoos: Defect and Diffusion Forum., 273-276 (2008) 329- 334.